ACS APPLIED MATERIALS & INTERFACES

Research Article

www.acsami.org

Carbon "Quantum" Dots for Fluorescence Labeling of Cells

Jia-Hui Liu,[†,‡,#] Li Cao,[‡,#] Gregory E. LeCroy,[‡] Ping Wang,[‡] Mohammed J. Meziani,[‡] Yiyang Dong,[†] Yuanfang Liu,[§,¶] Pengju G. Luo,[‡] and Ya-Ping Sun*[,‡]

[†]Beijing Key Laboratory of Bioprocess, College of Life Science and Technology, Beijing University of Chemical Technology, Beijing 100029, China

[‡]Department of Chemistry and Laboratory for Emerging Materials and Technology, Clemson University, Clemson, South Carolina 29634, United States

[§]Beijing National Laboratory for Molecular Sciences, College of Chemistry and Molecular Engineering, Peking University, Beijing 100871, China

[¶]Institute of Nanochemistry and Nanobiology, Shanghai University, Shanghai 200444, China

ABSTRACT: The specifically synthesized and selected carbon dots of relatively high fluorescence quantum yields were evaluated in their fluorescence labeling of cells. For the cancer cell lines, the cellular uptake of the carbon dots was generally efficient, resulting in the labeling of the cells with bright fluorescence emissions for both one- and two-photon excitations from predominantly the cell membrane and cytoplasm. In the exploration on labeling the live stem cells, the cellular uptake of the carbon dots was relatively less efficient, though fluorescence emissions could still be adequately detected in the labeled cells, with the emissions again predominantly from the cell membrane and cytoplasm. This combined with the observed more efficient internalization of the same carbon dots by the fixed stem cells might suggest some significant selectivity of the stem cells toward surface functionalities of the carbon dots. The needs and possible strategies for more systematic and comparative studies on the fluorescence labeling of different cells, including especially live stem cells, by carbon dots as a new class of brightly fluorescent probes are discussed.

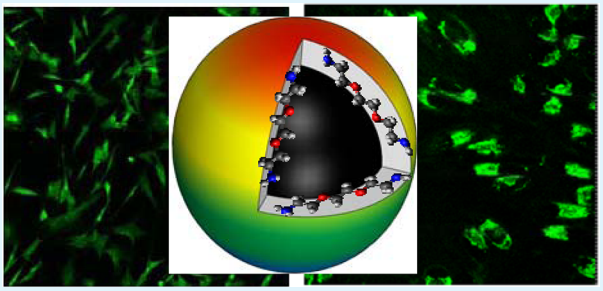

KEYWORDS: *carbon dots, fluorescence labeling, cell imaging, stem cells, two-photon fluorescence, quantum dots*

INTRODUCTION

Fluorescent semiconductor nanocrystals, commonly referred to as quantum dots (QDs), have attracted much attention for serving as probes in cell imaging and other biomedical applications.[1,2] Strong cases have been made in the literature for using QDs to replace organic dyes and in some applications genetically encoded fluorescent tags due to their advantages such as the fluorescence brightness at the individual dot level, photostability, and so on.[1−3] With a growing demand on high-performance fluorescence tags and probes for cell labeling and imaging purposes, much effort has been made to expand the offering of QD-like fluorescent nanomaterials beyond those based on conventional semiconductors. Among more significant recent successes have been the finding and subsequent development of carbon "quantum" dots or more appropriately called carbon dots (for the lack of the classical quantum confinement effect in these nanomaterials),[4−11] which have played a leading role in an emerging and rapidly expanding research field centered on the design, preparation, and potential biomedical uses of various carbon-based QDs.[12−25]

Carbon dots are generally small carbon nanoparticles with various surface passivation schemes by organic or biomolecules (Figure 1),[4,6,7,12] where the more effective surface passivation has been correlated with brighter fluorescence emissions from the corresponding dots. The optical absorption of carbon dots is assigned to π-plasmon transitions in the carbon nanoparticle core of the dots, while the fluorescence emissions in the visible to near-IR are attributed to photogenerated electrons and holes trapped at diverse surface sites and their associated radiative recombinations.[4,12] Carbon dots also have relatively very large

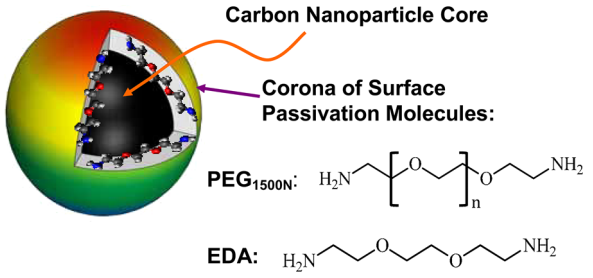

Figure 1. Cartoon illustration on carbon dot, which is generally a small carbon nanoparticle core with attached and strongly adsorbed surface passivation molecules (a configuration similar to a soft corona).

Received: June 26, 2015
Accepted: August 11, 2015
Published: August 11, 2015

DOI: 10.1021/acsami.5b05665
ACS Appl. Mater. Interfaces 2015, 7, 19439−19445

two-photon excitation cross sections in the near-IR (800−900 nm), with the resulting fluorescence emissions reported in the literature comparable roughly to those associated with the regular excitation into the optical absorption spectrum.[5,26−28] Nevertheless, for specimens of carbon dots on a substrate, colocalization experiments in which the same specimen was imaged with both one- and two-photon excitations on the same platform did confirm that the observed fluorescence emissions were associated with the same nanoscale entity.[5] Carbon dots have been found to be highly photochemically stable, without the optical blinking commonly observed in semiconductor QDs.[4] It is now generally acknowledged that carbon dots represent a new class of high-performance one- and two-photon fluorescence imaging agents.

According to results from various cytotoxicity assays, carbon dots in terms of the intrinsic material configuration are nontoxic to cells at concentration levels much higher than those commonly used for fluorescence labeling and imaging purposes.[6,7,29,30] Even at high concentrations, the effect of carbon dots on cells is mostly associated with the surface passivation agents, and interestingly, such agents in carbon dots are less cytotoxic than their free counterparts.[29,30] Therefore, there have been a number of experiments reported in the literature on carbon dots for fluorescence labeling and imaging of cells.[6−11] For example, Cao et al. used PEGylated carbon dots for the fluorescence imaging of human breast cancer MCF-7 cells with one- and two-photon excitations.[5] Zhang et al. prepared carbon dots from polydopamine for cell imaging. At 405 and 458 nm excitations, green and yellow fluorescence emissions, respectively, were observed in the cytoplasm but not in the cell nucleus.[31] Chen et al. prepared carbon dots by carbonizing sucrose with oil acid for imaging 16HBE cells. Green fluorescence emissions were observed around the cell membrane, in addition to the cytoplasm, though only much weaker fluorescence was detected in the cell nucleus.[32] More recently, Yang et al. conjugated hydrothermally synthesized carbon dots with nuclear localization signal (NLS) peptides for the fluorescence imaging of MCF-7 and A549 cells.[33] While some accumulation within the cell nucleus was detected, the majority of the carbon dots were found to be residing in the cytoplasm and cell membrane.[33] However, most of the reported studies might be considered as being exploratory in nature, and more experiments based on carbon dots of more desirable properties (very bright fluorescence emissions, compactness, etc.) are still needed, especially for broader applications to include stem cells and other special cell lines. In the work reported here, we evaluated the specifically selected carbon dots of relatively high fluorescence quantum yields (with respect to one-photon excitation in the visible spectral region) in their labeling of cancer cell lines under one- and two-photon excitation conditions, and we also explored the labeling of stem cells with the carbon dots. For the latter especially, the results concerning the effect of surface functionalities in carbon dots on the cell labeling efficiency are highlighted and discussed.

EXPERIMENTAL SECTION

Materials. Carbon nanopowder (<50 nm, purity >99%) and 2,2′-(ethylenedioxy)bis(ethylamine) (EDA) were purchased from Sigma-Aldrich, and bis(3-aminopropyl)-terminated oligomeric poly(ethylene glycol) of average molecular weight ∼1500 (PEG_{1500N}) was from Anvia Chemicals. Thionyl chloride (>99%) was obtained from Alfa Aesar, nitric acid from VWR, and Sephadex G-100 gel from GE Healthcare. Dialysis membrane tubing of various cutoff molecular weights was supplied by Spectrum Laboratories. Water was deionized and purified by being passed through a Labconco WaterPros water purification system.

Measurement. Baxter Megafuge (model 2630), Eppendorf (model 5417 R), and Beckman-Coulter ultracentrifuge (Optima L90K with a type 90 Ti fixed-angle rotor) were used for centrifugation at various *g* values. Optical absorption spectra were recorded on a Shimadzu UV2501-PC spectrophotometer. Fluorescence spectra were measured on a Jobin-Yvon emission spectrometer equipped with a 450 W xenon source, Gemini-180 excitation and Tirax-550 emission monochromators, and a photon counting detector (Hamamatsu R928P PMT at 950 V). Fluorescence quantum yields were measured in reference to 9,10-bis(phenylethynyl)-anthracene as a standard (quantum yield of unity, calibrated against the quinine sulfate standard). NMR measurements were performed on a Bruker Avance 500 NMR spectrometer. Transmission electron microscopy (TEM) images were obtained on a Hitachi H9500 TEM system. A Leica laser scanning confocal fluorescence microscope (DM IRE2, with Leica TCS SP2 SE scanning system) equipped with an argon ion laser (JDS Uniphase) and a femtosecond pulsed Ti:sapphire laser (Spectra-Physics Tsunami with a 5 W Millennia pump) was used in the imaging experiments, so was a Zeiss LSM 700 laser scanning microscope. On both microscopes, a plan apochromat 100× oil immersion objective was used. The images were processed and analyzed with the NIH ImageJ software.

Carbon Dots. For carbon nanoparticles as the precursor for carbon dots, an as-supplied carbon nanopowder sample (1 g) was refluxed in an aqueous nitric acid solution (5 M, 90 mL) for 48 h. The reaction mixture was cooled back to ambient temperature and then dialyzed against fresh water for up to 3 days. The postdialysis mixture was centrifuged at 1000*g* to retain the supernatant, followed by the removal of water to obtain the desired carbon nanoparticle sample.

In the synthesis of PEG_{1500N}-carbon dots, the carbon nanoparticle sample obtained from the processing above was refluxed in neat thionyl chloride for 12 h, followed by the removal of excess thionyl chloride under nitrogen. The post-treatment carbon nanoparticle sample (100 mg) was mixed well with carefully dried PEG_{1500N} (1 g) in a flask, heated to 110 °C, and stirred at the constant temperature under nitrogen for 72 h. The reaction mixture was cooled to ambient temperature, dispersed in water, and then centrifuged at 20 000*g* to retain the dark supernatant as an aqueous solution of the as-prepared PEG_{1500N}-carbon dots.

The EDA-carbon dots were synthesized in largely the same experimental procedures as those described above. The post-thionyl chloride treatment carbon nanoparticle sample (50 mg) was mixed well with carefully dried EDA liquid (600 mg) in a round-bottom flask, heated to 120 °C, and vigorously stirred under nitrogen protection for 3 days. The reaction mixture was cooled back to ambient temperature, dispersed in water, and then centrifuged at 20 800*g* to retain the supernatant as an aqueous solution of the as-prepared EDA-carbon dots.

The as-prepared PEG_{1500N}-carbon dots and EDA-carbon dots samples were filtrated through a Sephadex G-100 gel column for fractionation. The gel column was packed in house with commercially supplied gel sample and evaluated according to protocols already reported in the literature.[34] For PEG_{1500N}-carbon dots, more fluorescent fractions eluted from the gel column were collected and combined to have the resulting sample in sufficient quantity and a fluorescence quantum yield of ∼40% at 440 nm excitation. For EDA-carbon dots, the colored section on the gel column with high fluorescence quantum yields was collected, followed by dialysis against fresh water (dialysis tubing cutoff molecular weight ∼500) to obtain the desired sample, whose ^{1}H and ^{13}C NMR spectra were similar to those reported previously.[20]

Cells and Imaging. The human breast cancer cell line MCF-7 (ATCC) and human colon adenocarcinoma grade II cell line HT-29 (ATCC) were grown at 37 °C with 5% CO_2 in EMEM medium (ATCC, with nonessential amino-acids, 1 mM sodium pyruvate, 2 mM L-glutamine, and 1.5 g/L sodium bicarbonate) supplemented with 10% (v/v) fetal bovine serum (ATCC) and 1% of penicillin/streptomycin

DOI: 10.1021/acsami.5b05665
ACS Appl. Mater. Interfaces 2015, 7, 19439−19445

(Cambrex Bio Science). The cells were plated on a four-chambered Lab-Tek cover-glass system (Nalge Nunc) at 50 000 cells per chamber for 24 h. Separately, the selected carbon dots in aqueous solutions were diluted to the desired concentrations with fresh culture medium and sterilized with a 0.2 μm Acrodisc syringe filter just prior to the cell exposure, and the samples were introduced to the cells. Cells cultured in the free medium were taken as the control. Upon incubation for up to 24 h, the cells were washed three times with PBS (500 μL each time) and kept in PBS for fluorescence imaging. The confocal fluorescence images were obtained with 405 or 458 nm excitation, and the two-photon images were acquired with femtosecond pulsed laser excitation at 800−900 nm.

The SD rat mesenchymal stem cells (MSCs) from passage 2 (OriCell Sprague−Dawley rat MSCs, Cyagen) were expanded in SD rat MSC basal media with 10% fetal bovine serum and 1% v/v penicillin/streptomycin. The MSCs within passage 8 were used in all experiments. For the viability assay, the cells were plated in 96-well plates at an initial density of 1×10^4 cells per well in 200 μL of growth medium for incubation. The EDA-carbon dots were diluted with fresh culture medium to the exposure concentrations, and the solutions were introduced to the cells. The cells cultured in the free medium were taken as the control. Upon the exposure for 24 h, the cell viability was determined by using the Cell Counting Kit-8 (CCK-8, Dojindo Laboratory) assay.

For the labeling, the stem cells were plated on a four-chambered Lab-Tek cover-glass system (Nalge Nunc) at 50 000 cells per chamber for 24 h, followed by their being mixed with the separately prepared carbon dots sample. For the EDA-carbon dots, the sample preparation included the treatment with aqueous HCl for the pH to be neutral before the sample solution was used for labeling the MSCs. In another set of experiments, the MSCs were plated on a four-chambered Lab-Tek cover-glass system for 24 h and fixed by 4% formaldehyde, followed by being mixed with the separately prepared carbon dots sample. Upon incubation for up to 24 h, the live or fixed cells were washed carefully with PBS for a complete removal of unattached carbon dots, and the cells postwashing were kept in PBS for the imaging experiments. The confocal fluorescence images were obtained with 405 nm excitation. For a more quantitative comparison of the signal intensities in the images, the as-acquired color fluorescence images were converted to the grayscale by using the ImageJ software (NIH). The images were then mapped digitally for a determination of the corresponding fluorescence intensities.

RESULTS AND DISCUSSION

The PEG_{1500N}-carbon dots and EDA-carbon dots were synthesized as reported previously.[19,20,34] The as-synthesized samples were separated on an aqueous Sephadex G-100 gel column, from which more fluorescent fractions were collected. Shown in Figure 2 are absorption and fluorescence spectra of the PEG_{1500N}-carbon dots and EDA-carbon dots that were used in cell imaging experiments, with the fluorescence quantum yields of the two samples at 440 nm excitation of ~40% and ~30%, respectively. These carbon dots are generally small in size, as confirmed by results from microscopy analyses (Figure 3),[20,34] especially so for the EDA-carbon dots characterized as being "ultracompact" due to the much shorter PEG chain in EDA than that in PEG_{1500N}.[20]

The carbon dots in aqueous solution were progressively diluted for being deposited onto a substrate (glass slide) to have them individually dispersed for fluorescence imaging under single-dot conditions. The fluorescence of the specimen could readily be detected under a confocal microscope, with the observed images confirming the desired dispersion of the carbon dots (Figure 4).

The specimens of PEG_{1500N}-carbon dots were also imaged with two-photon excitation at 800 nm, in which fluorescence emissions were readily detected, again confirming the desired

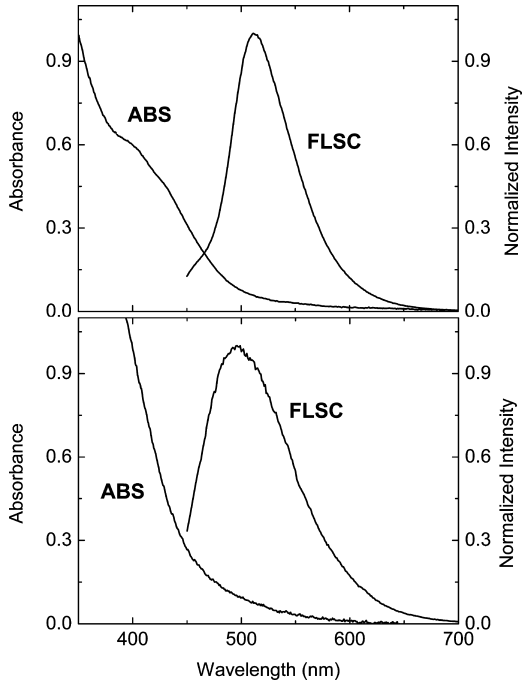

Figure 2. Absorption (ABS) and fluorescence (FLSC, 440 nm excitation) spectra of the PEG_{1500N}-carbon dots (top) and EDA-carbon dots (bottom) in aqueous solutions.

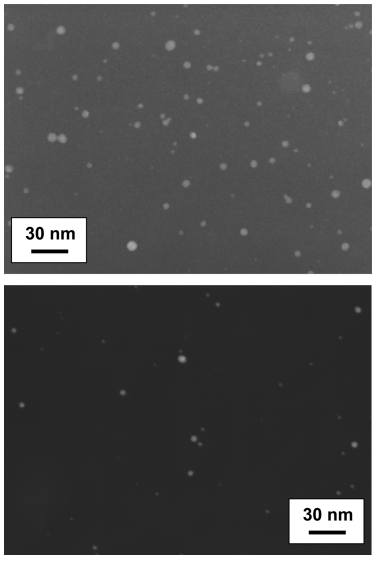

Figure 3. TEM images of the PEG_{1500N}-carbon dots (top) and EDA-carbon dots (bottom).

dispersion of carbon dots on the substrate (Figure 5). The fluorescence spectra corresponding to the individualized dot images were collected on the microscope for comparison with the solution-phase spectra of the carbon dots measured on a conventional emission spectrometer at corresponding excitation wavelengths (800 nm two-photon vs 400 nm one-photon). The results suggested that the spectra were comparable qualitatively (Figure 5), reflecting not only their likelihood of being from the same emissive excited states but also the comparability between the fluorescence properties of the carbon dots in solution and when dispersed on a substrate under single-dot conditions.

DOI: 10.1021/acsami.5b05665
ACS Appl. Mater. Interfaces 2015, 7, 19439−19445

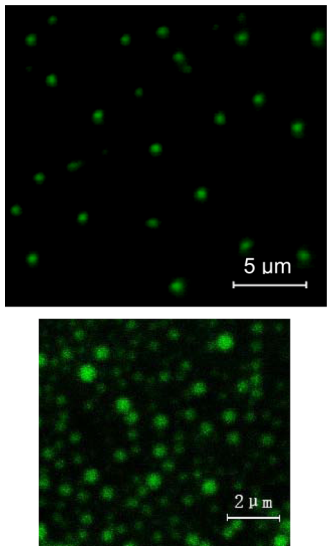

Figure 4. Confocal fluorescence images of the PEG_{1500N}-carbon dots (top) and EDA-carbon dots (bottom) well-dispersed on a glass substrate.

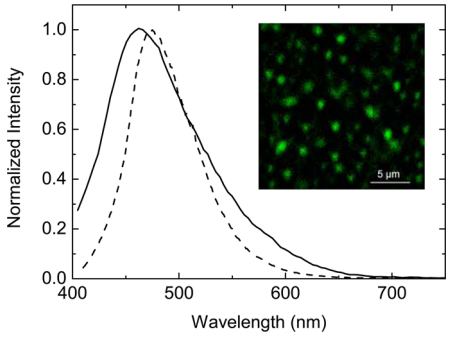

Figure 5. Comparison of the fluorescence spectrum (two-photon excitation at 800 nm) of an individually dispersed PEG_{1500N}-carbon dot on a glass substrate (solid line) with that (regular fluorescence spectrometer at 400 nm excitation) of the corresponding dots in aqueous solution (dashed line). Inset: Two-photon fluorescence images (800 nm excitation) of the PEG_{1500N}-carbon dots.

The results highlighted above for the PEG_{1500N}-carbon dots and EDA-carbon dots of relatively high fluorescence quantum yields suggest that these are well-behaved fluorescence probes in the visible spectral region for both one- and two-photon excitations. These probes are generally stable in their optical absorption and fluorescence properties in various aqueous buffers, amenable to cell labeling and imaging applications.

The human breast cancer MCF-7 and human colon adenocarcinoma HT-29 cells were selected for the labeling by the PEG_{1500N}-carbon dots. Both MCF-7 and HT-29 cells were cultured by following established protocols.[29,30] For the cell imaging experiments, the cells were incubated with the PEG_{1500N}-carbon dots in an aqueous buffer at 37 °C for up to 24 h and then washed to remove carbon dots that were not associated with the cells. Since the dot concentrations were significantly lower than those that could cause cell damage,[30] the cells were close to completely viable under the experimental conditions.

For both cell lines, the fluorescence images acquired with 458 nm excitation (argon ion laser line) suggested significant uptake of the carbon dots by the cells, with the dots mostly residing in the cell membrane and cytoplasm and without any meaningful presence in the cell nucleus (Figure 6). There were no major

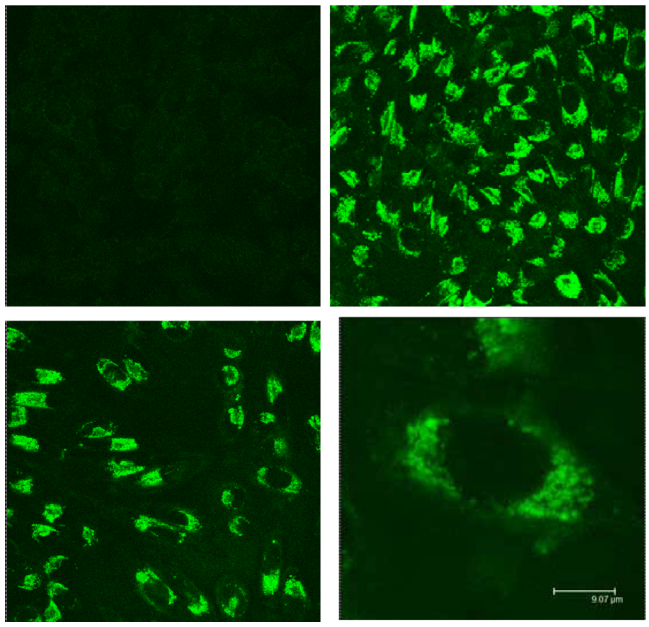

Figure 6. Confocal fluorescence images (458 nm excitation, 470−590 nm emissions) for MCF-7 cells without (top left) and with the PEG_{1500N}-carbon dots (top right) and for HT-29 cells with the PEG_{1500N}-carbon dots at different resolutions (bottom left and right).

differences between the two cell lines in terms of their fluorescence labeling by the carbon dots. The contrast between the emissive carbon dots and the background (somewhat fluorescent in general) was very good, due likely to the high fluorescence quantum yields of the carbon dots used for the cell labeling. For an estimate of the fluorescence brightness in the labeled cells, while using an established standard as intensity reference was rather difficult in our setup and therefore not pursued, qualitatively the brightness in the fluorescence images of the cells was comparable with that in the images of the carbon dots without cells. It suggests that the fluorescence properties of the carbon dots were not degraded in any significant fashion upon their being taken up by the cells. In fact, there is experimental evidence from unrelated studies on the carbon dots in polymer films indicating enhanced fluorescence intensities for the dots in a more confined environment. The possibility for similar effects on carbon dots in various cellular domains will be evaluated in further investigations.

The same cells labeled with the PEG_{1500N}-carbon dots were imaged by using the fluorescence microscope with two-photon excitation (femtosecond pulsed laser at 800−900 nm) under otherwise the same experimental conditions. Green fluorescence emissions from the PEG_{1500N}-carbon dots in both cell lines could readily be detected, with the results again suggesting that the dots resided mostly in the cell membrane and cytoplasm and no major differences between the two cell lines (Figure 7). Two-photon fluorescence imaging has been widely acknowledged as being particularly advantageous in terms of minimizing background fluorescence interferences, though in this case the advantage was not so obvious. The imaging contrast appeared not so different from that found in one-photon (regular confocal, Figure 6) experiments, as both were

DOI: 10.1021/acsami.5b05665
ACS Appl. Mater. Interfaces 2015, 7, 19439−19445

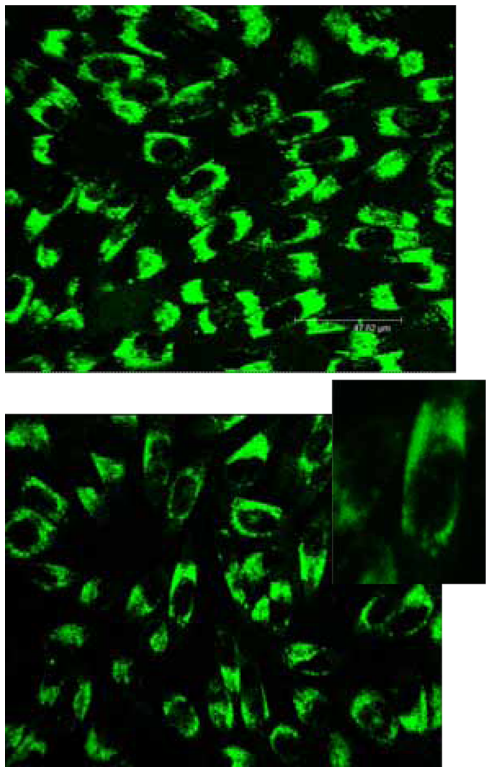

Figure 7. Fluorescence images with two-photon excitation (800 nm excitation, 470−590 nm emissions) for MCF-7 (top) and HT-29 (bottom, and the inset) cells, both labeled with the PEG_{1500N}-carbon dots.

relatively high, again due likely to the high fluorescence quantum yields of the carbon dots used for the cell labeling. There was more experimental evidence supporting the dependence of labeling and imaging outcomes on the quality of the carbon dots. For example, when another PEG_{1500N}-carbon dots sample of a lower fluorescence quantum yield (~6% at 440 nm excitation, a fraction from the aqueous gel column separation of the as-synthesized sample) was used for labeling the same cells under otherwise the same experimental conditions, the fluorescence intensities in the resulting images were obviously lower, as expected.

In the fluorescence labeling of cells with the carbon dots, the efficiency as reflected by the brightness and contrast in the images obtained with one- and two-photon excitations was clearly dependent on incubation conditions, especially the length of time in which the cells were exposed to the carbon dots. Under otherwise the same experimental conditions, the longer incubation time (24 h vs 6 h, for example) resulted in more effective fluorescence labeling of the cells, corresponding to significantly brighter and higher-contrast images of the resulting cell specimens. The cellular uptake of the carbon dots was essentially absent when the incubation was at low temperature (4 °C), as reported previously.[5]

Beyond the human cancer cells, the carbon dots were also explored for their labeling of mesenchymal stem cells (MSCs). As a justification, stem cells are widely considered as holding the promise for a variety of *in vivo* tracking applications. Fluorescence probes are in demand for labeling stem cells[35] due to some advantageous attributes over those of other labels, such as magnetic and Raman probes.[36−38] In addition to the high sensitivity associated with bright fluorescence emissions in the probes for stem cells, these probes are also required to minimally affect the subcellular structure and have no or little toxic effect.[39,40] For conventional semiconductor QDs as fluorescence probes, it was found that those functionalized with long ligands were more cytotoxic than those with short ligands.[41] The EDA-carbon dots in this work were developed specifically as bright fluorescence probes of an ultracompact configuration for related purposes,[20] and they were used in the labeling of MSCs.

Experimentally, the SD rat MSCs within passage 8 were used in the cell labeling experiments with the EDA-carbon dots. The results from the cell viability assay suggested that the stem cells were completely viable upon being exposed to the EDA-carbon dots at concentrations much higher than those used in the fluorescence labeling under otherwise the same experimental conditions. In the labeling evaluation, postexposure of the stem cells to the separately prepared EDA-carbon dots, the cells were imaged under a confocal fluorescence microscope with 405 nm excitation. The fluorescence images thus obtained confirmed the labeling of the stem cells by the carbon dots (Figure 8),

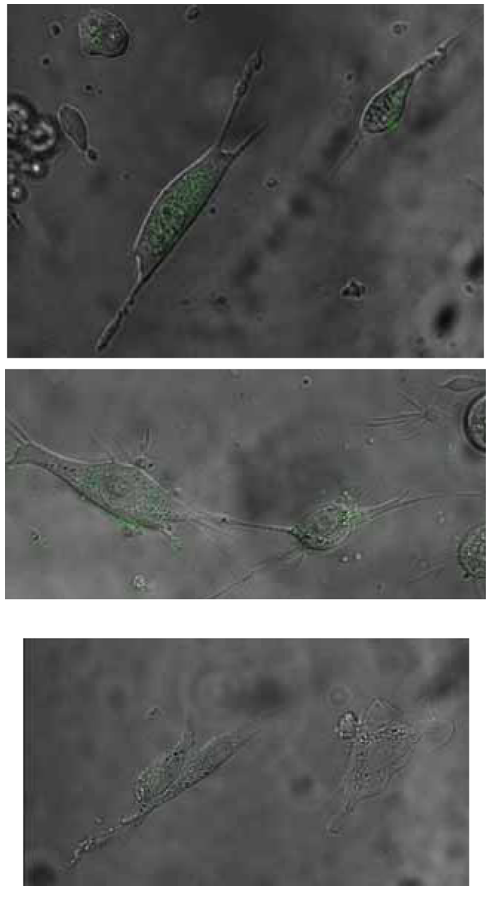

Figure 8. Merged (fluorescence + bright-field) images of the live stem cells labeled with the EDA-carbon dots (top and middle) and the control (without the dots, bottom).

suggesting that the dots in the live cells were again mostly in the cell membrane and cytoplasm, not in the nucleus, similar in general to the cellular distribution of the other PEGylated carbon dots in human cancer cells MCF-7 and HT-29 described above. However, the labeling efficiency for the stem cells by the EDA-carbon dots was significantly lower, as reflected in the low cellular uptake of the carbon dots and

DOI: 10.1021/acsami.5b05665
ACS Appl. Mater. Interfaces 2015, 7, 19439−19445

weaker fluorescence emissions in the images. One possible cause might be related to the chemical structures of EDA-carbon dots, which are rather basic (pH ~ 13) due to a relatively large population of amino groups on the dot surface (Figure 1). Consequently, aqueous EDA-carbon dots sample had to be neutralized with an acid (aqueous HCl) before the stem cell labeling. The acid treatment protonated the amino groups to result in a similarly large population of cationic moieties on the dot surface, which were probably not favorable to the desired efficient uptake by the live cells. In a follow-up exploration on this issue, the MSCs were fixed by the treatment with 4% formaldehyde. The labeling of the fixed MSCs by the EDA-carbon dots was much more efficient, corresponding to much brighter fluorescence images and with the hyperchromatic nucleolus brighter than the other regions (Figure 9). Here, a quantification of the fluorescence brightness was

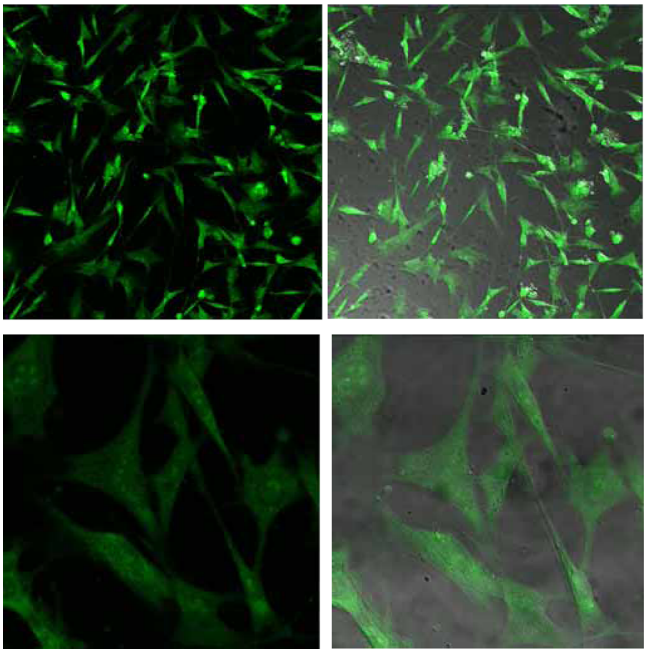

Figure 9. Fluorescence (left) and merged (fluorescence + bright-field, right) images of the fixed stem cells labeled with the EDA-carbon dots.

accomplished by converting the as-acquired color images into the grayscale (NIH ImageJ software), followed by mapping the resulting images digitally to determine the spatially resolved fluorescence intensities.

The results described above suggested that the live MSCs could be labeled by the EDA-carbon dots, but the labeling efficiency was relatively low, insufficient for being used in following the cell divisions (such as in the 20 day cell division or differentiation culture). Further investigations with the design and synthesis of brightly fluorescent and compact carbon dots of surface functionalities more favorable to the uptake by live stem cells will be pursued. Also, a comparison between stem cells and commonly studied cancer cell lines (those used in this study and others such as Hela cells) with respect to carbon dots of the same surface functionalities will be investigated. It seems that stem cells are more "picky" about surface functionalities when taking up the carbon dots, as cancer and other cell lines often used in the literature on carbon dots have not exhibited in general the kind of issues with a high population of amino moieties on the dot surface affecting cellular uptake. This presents both challenges and opportunities in the use of carbon dots as a new class of fluorescence probes for the labeling of stem cells, with the latter enabling potentially the exploitation of selectivity in the uptake of the probes by stem cells vs other cell lines.

CONCLUSION

The carbon dots of bright fluorescence emissions can be synthesized in a relatively facile fashion, and they can be imaged down to the individual dot level on a substrate by using both one- and two-photon excitations. The uptake of the carbon dots by cancer cells is generally efficient, resulting in the labeling of the cells with bright fluorescence from predominantly the cell membrane and cytoplasm, again with both one- and two-photon excitations. In the use of the ultracompact EDA-carbon dots for labeling live stem cells, the cellular uptake is relatively less efficient, though the fluorescence emissions can still be adequately detected and they are again predominantly from the cell membrane and cytoplasm. This combined with the observed more efficient internalization of the same carbon dots by the fixed stem cells may suggest selectivity of the live stem cells toward the dot surface functionalities. More systematic and comparative studies on the fluorescence labeling of different cell lines by carbon dots, including more specific design and synthesis of carbon dots that are more suitable for the labeling of stem cells, are needed and will be pursued.

AUTHOR INFORMATION

Corresponding Author

*E-mail: syaping@clemson.edu.

Author Contributions

#J.-H.L. and L.C. contributed equally.

Notes

The authors declare no competing financial interest.

ACKNOWLEDGMENTS

J.-H.L. acknowledges financial support by China Natural Science Foundation (No. 21301015), and Y.-P.S. acknowledges support from NIH and NSF. L.C. was funded by a *Susan G. Komen for the Cure* Postdoctoral Fellowship, and M.J.M. was on leave from Department of Chemistry and Physics, Northwest Missouri State University with support provided by the South Carolina Space Grant Consortium.

REFERENCES

(1) Kairdolf, B. A.; Smith, A. M.; Stokes, T. H.; Wang, M. D.; Young, A. N.; Nie, S. Semiconductor Quantum Dots for Bioimaging and Biodiagnostic Applications. *Annu. Rev. Anal. Chem.* **2013**, *6*, 143−162.

(2) Freeman, R.; Willner, I. Optical Molecular Sensing with Semiconductor Quantum Dots (QDs). *Chem. Soc. Rev.* **2012**, *41*, 4067−4085.

(3) Medintz, I. L.; Uyeda, H. T.; Goldman, E. R.; Mattoussi, H. Quantum Dot Bioconjugates for Imaging, Labelling and Sensing. *Nat. Mater.* **2005**, *4*, 435−546.

(4) Sun, Y.-P.; Zhou, B.; Lin, Y.; Wang, W.; Fernando, K. A. S.; Pathak, P.; Meziani, M. J.; Harruff, B. A.; Wang, X.; Wang, H.; Luo, P. G.; Yang, H.; Kose, M. E.; Chen, B.; Veca, M.; Xie, S. Y. Quantum-Sized Carbon Dots for Bright and Colorful Photoluminescence. *J. Am. Chem. Soc.* **2006**, *128*, 7756−7757.

(5) Cao, L.; Wang, X.; Meziani, M. J.; Lu, F.; Wang, H.; Luo, P. G.; Lin, Y.; Harruff, B. A.; Veca, L. M.; Murray, D.; Xie, S. Y.; Sun, Y.-P. Carbon Dots for Multiphoton Bioimaging. *J. Am. Chem. Soc.* **2007**, *129*, 11318−11319.

DOI: 10.1021/acsami.5b05665
ACS Appl. Mater. Interfaces 2015, 7, 19439−19445

(6) Luo, P. G.; Sahu, S.; Yang, S.-T.; Sonkar, S. K.; Wang, J.; Wang, H.; LeCroy, G. E.; Cao, L.; Sun, Y.-P. Carbon "Quantum" Dots for Optical Bioimaging. *J. Mater. Chem. B* **2013**, *1*, 2116−2127.
(7) Luo, P. G.; Sonkar, S. K.; Yang, S.-T.; Yang, F.; Yang, L.; Broglie, J. J.; Liu, Y.; Sun, Y.-P. Carbon-Based Quantum Dots for Fluorescence Imaging of Cells and Tissues. *RSC Adv.* **2014**, *4*, 10791−10807.
(8) Wang, Y.; Hu, A. Carbon Quantum Dots: Synthesis, Properties and Applications. *J. Mater. Chem. C* **2014**, *2*, 6921−6939.
(9) Lim, S. Y.; Shen, W.; Gao, Z. Carbon Quantum Dots and Their Applications. *Chem. Soc. Rev.* **2015**, *44*, 362−381.
(10) Miao, P.; Han, K.; Tang, Y.; Wang, B.; Lin, T.; Cheng, W. Recent Advances in Carbon Nanodots: Synthesis, Properties and Biomedical Applications. *Nanoscale* **2015**, *7*, 1586−1595.
(11) Zhao, A.; Chen, Z.; Zhao, C.; Gao, N.; Ren, J.; Qu, X. Recent Advances in Bioapplications of C-dots. *Carbon* **2015**, *85*, 309−327.
(12) Cao, L.; Meziani, M. J.; Sahu, S.; Sun, Y.-P. Photoluminescence Properties of Graphene versus Other Carbon Nanomaterials. *Acc. Chem. Res.* **2013**, *46*, 171−180.
(13) Hola, K.; Zhang, Y.; Wang, Y.; Giannelis, E. P.; Zboril, R.; Rogach, A. L. Carbon Dots-Emerging Light Emitters for Bioimaging, Cancer Therapy and Optoelectronics. *Nano Today* **2014**, *9*, 590−603.
(14) Yang, S.-T.; Cao, L.; Luo, P. G.; Lu, F.; Wang, X.; Wang, H.; Meziani, M. J.; Liu, Y.; Qi, G.; Sun, Y.-P. Carbon Dots for Optical Imaging in Vivo. *J. Am. Chem. Soc.* **2009**, *131*, 11308−11309.
(15) Zhang, J.; Shen, W.; Pan, D.; Zhang, Z.; Fang, Y.; Wu, M. Controlled Synthesis of Green and Blue Luminescent Carbon Nanoparticles with High Yields by the Carbonization of Sucrose. *New J. Chem.* **2010**, *34*, 591−593.
(16) Anilkumar, P.; Wang, X.; Cao, L.; Sahu, S.; Liu, J.-H.; Wang, P.; Korch, K.; Tackett, K. N.; Parenzan, A.; Sun, Y.-P. Toward Quantitatively Fluorescent Carbon-Based "Quantum" Dots. *Nanoscale* **2011**, *3*, 2023−2027.
(17) Wang, F.; Xie, Z.; Zhang, H.; Liu, C. Y.; Zhang, Y. G. Highly Luminescent Organosilane-Functionalized Carbon Dots. *Adv. Funct. Mater.* **2011**, *21*, 1027−1031.
(18) Cao, L.; Yang, S.-T.; Wang, X.; Luo, P. G.; Liu, J.-H.; Sahu, S.; Liu, Y.; Sun, Y.-P. Competitive Performance of Carbon "Quantum" Dots in Optical Bioimaging. *Theranostics* **2012**, *2*, 295−301.
(19) Anilkumar, P.; Cao, L.; Yu, J. J.; Tackett, K. N.; Wang, P.; Meziani, M. J.; Sun, Y.-P. Crosslinked Carbon Dots as Ultra-Bright Fluorescence Probes. *Small* **2013**, *9*, 545−551.
(20) LeCroy, G. E.; Sonkar, S. K.; Yang, F.; Veca, L. M.; Wang, P.; Tackett, K. N.; Yu, J. J.; Vasile, E.; Qian, H. J.; Liu, Y. M.; Luo, P.; Sun, Y.-P. Toward Structurally Defined Carbon Dots as Ultracompact Fluorescent Probes. *ACS Nano* **2014**, *8*, 4522−4529.
(21) Ding, C.; Zhu, A.; Tian, Y. Functional Surface Engineering of C-Dots for Fluorescent Biosensing and in Vivo Bioimaging. *Acc. Chem. Res.* **2014**, *47*, 20−30.
(22) Lemenager, G.; de Luca, E.; Sun, Y.-P.; Pompa, P. P. Super-Resolution Fluorescence Imaging of Biocompatible Carbon Dots. *Nanoscale* **2014**, *6*, 8617−8626.
(23) Weng, C. I.; Chang, H. T.; Lin, C. H.; Shen, Y. W.; Unnikrishnan, B.; Li, Y. J.; Huang, C. C. One-Step Synthesis of Biofunctional Carbon Quantum Dots for Bacterial Labeling. *Biosens. Bioelectron.* **2015**, *68*, 1−6.
(24) Bao, L.; Liu, C.; Zhang, Z. L.; Pang, D. W. Photoluminescence-Tunable Carbon Nanodots: Surface-State Energy-Gap Tuning. *Adv. Mater.* **2015**, *27*, 1663−1667.
(25) Pei, S.; Zhang, J.; Gao, M.; Wu, D.; Yang, Y.; Liu, R. A Facial Hydrothermal Approach towards Photoluminescent Carbon Dots from Amino Acids. *J. Colloid Interface Sci.* **2015**, *439*, 129−133.
(26) Kong, B.; Zhu, A.; Ding, C.; Zhao, X.; Li, B.; Tian, Y. Carbon Dot-Based Inorganic-Organic Nanosystem for Two-Photon Imaging and Biosensing of pH Variation in Living Cells and Tissues. *Adv. Mater.* **2012**, *24*, 5844−5848.
(27) Zhu, A.; Luo, Z.; Ding, C.; Li, B.; Zhou, S.; Wang, R.; Tian, Y. A Two-Photon ″Turn-on″ Fluorescent Probe Based on Carbon Nanodots for Imaging and Selective Biosensing of Hydrogen Sulfide in Live Cells and Tissues. *Analyst* **2014**, *139*, 1945−1952.
(28) Tong, G.; Wang, J.; Wang, R.; Guo, X.; He, L.; Qiu, F.; Wang, G.; Zhu, B.; Zhu, X.; Liu, T. Amorphous Carbon Dots with High Two-Photon Fluorescence for Cellular Imaging Passivated by Hyperbranched Poly(amino amine). *J. Mater. Chem. B* **2015**, *3*, 700−706.
(29) Yang, S.-T.; Wang, X.; Wang, H.; Lu, F.; Luo, P. G.; Cao, L.; Meziani, M. J.; Liu, J.-H.; Liu, Y.; Chen, M.; Huang, Y.; Sun, Y.-P. Carbon Dots as Nontoxic and High-Performance Fluorescence Imaging Agents. *J. Phys. Chem. C* **2009**, *113*, 18110−18114.
(30) Wang, Y.; Anilkumar, P.; Cao, L.; Liu, J.-H.; Luo, P. G.; Tackett, K. N.; Sahu, S.; Wang, P.; Wang, X.; Sun, Y.-P. Carbon Dots of Different Composition and Surface Functionalization - Cytotoxicity Issues Relevant to Fluorescence Imaging of Cells. *Exp. Biol. Med. (London, U. K.)* **2011**, *236*, 1231−1238.
(31) Zhang, X.; Wang, S.; Xu, L.; Ji, Y.; Feng, L.; Tao, L.; Li, S.; Wei, Y. Biocompatible Polydopamine Fluorescent Organic Nanoparticles: Facile Preparation and Cell Imaging. *Nanoscale* **2012**, *4*, 5581−5584.
(32) Chen, B.; Li, F.; Li, S.; Weng, W.; Guo, H.; Guo, T.; Zhang, H.; Chen, Y.; Huang, T.; Hong, X.; You, S.; Lin, Y.; Zeng, K.; Chen, S. Large Scale Synthesis of Photoluminescent Carbon Nanodots and Their Application for Bioimaging. *Nanoscale* **2013**, *5*, 1967−1971.
(33) Yang, L.; Jiang, W.; Qiu, L.; Jiang, X.; Zuo, D.; Wang, D.; Yang, L. One Pot Synthesis of Highly Luminescent Polyethylene Glycol Anchored Carbon Dots Functionalized with a Nuclear Localization Signal Peptide for Cell Nucleus Imaging. *Nanoscale* **2015**, *7*, 6104−6113.
(34) Wang, X.; Cao, L.; Yang, S.-T.; Lu, F.; Meziani, M. J.; Tian, L.; Sun, K. W.; Bloodgood, M. A.; Sun, Y.-P. Bandgap-Like Strong Fluorescent in Functionalized Carbon Nanoparticles. *Angew. Chem., Int. Ed.* **2010**, *49*, 5310−5314.
(35) Zhang, M.; Bai, L.; Shang, W.; Xie, W.; Ma, H.; Fu, Y.; Fang, D.; Sun, H.; Fan, L.; Han, M.; Liu, C.; Yang, S. Paper Facile Synthesis of Water-Soluble, Highly Fluorescent Graphene Quantum Dots as a Robust Biological Label for Stem Cells. *J. Mater. Chem.* **2012**, *22*, 7461−7467.
(36) Michalet, X.; Pinaud, F. F.; Bentolila, L. A.; Tsay, J. M.; Doose, S.; Li, J. J.; Sundaresan, G.; Wu, A. M.; Gambhir, S. S.; Weiss, S. Quantum Dots for Live Cells, in Vivo Imaging, and Diagnostics. *Science* **2005**, *307*, 538−544.
(37) Zhang, S. J.; Wu, J. C. Comparison of Different Imaging Techniques for Tracking Cardiac Stem Cell Therapy. *J. Nucl. Med.* **2007**, *48*, 1916−1919.
(38) Wang, Y.; Xu, C. J.; Ow, H. W. Commercial Nanoparticles for Stem Cell Labeling and Tracking. *Theranostics* **2013**, *3*, 544−560.
(39) Liang, C.; Wang, C.; Liu, Z. Stem Cell Labeling and Tracking with Nanoparticles. *Part. Part. Syst. Charact.* **2013**, *30*, 1006−1017.
(40) Shang, W. H.; Zhang, X. Y.; Zhang, M.; Fan, Z.; Sun, Y.; Han, M.; Fan, L. Z. The Uptake Mechanism and Biocompatibility of Graphene Quantum Dots with Human Neural Stem Cells. *Nanoscale* **2014**, *6*, 5799−5806.
(41) Nagy, A.; Steinbruck, A.; Gao, J.; Doggett, N.; Hollingsworth, J. A.; Iyer, R. Comprehensive Analysis of the Effects of CdSe Quantum Dot Size, Surface Charge, and Functionalization on Primary Human Lung Cells. *ACS Nano* **2012**, *6*, 4748−4762.

DOI: 10.1021/acsami.5b05665
ACS Appl. Mater. Interfaces 2015, 7, 19439−19445